

Long-Range Vibrational Dynamics are Directed by Watson-Crick Base-Pairing in Duplex DNA

Gordon Hithell,[†] Daniel J. Shaw,[†] Paul M. Donaldson,[‡] Gregory M. Greetham,[‡] Michael Towrie,[‡] Glenn A. Burley,[§] Anthony W. Parker,[‡] Neil T. Hunt^{*†}

[†]Department of Physics, University of Strathclyde, SUPA, 107 Rottenrow East, Glasgow, G4 0NG, UK

[‡]STFC Central Laser Facility, Research Complex at Harwell, Harwell Science and Innovation Campus, Didcot, OX11 0QX, UK

[§]Department of Pure and Applied Chemistry, University of Strathclyde, 295 Cathedral Street, Glasgow, G1 1XL, UK

Supporting Information Placeholder

ABSTRACT: Ultrafast two-dimensional infrared (2D-IR) spectroscopy of a 15-mer A-T DNA duplex in solution has revealed structure-dependent vibrational coupling and energy transfer processes linking bases with the sugar-phosphate backbone. Duplex melting induces significant changes in the positions of off-diagonal peaks linking carbonyl and ring-stretching vibrational modes of the adenine and thymine bases with vibrations of the phosphate group and phosphodiester linkage. These indicate that Watson-Crick hydrogen bonding and helix formation leads to a unique vibrational coupling arrangement of base vibrational modes with those of the phosphate unit. Based on observations from time-resolved 2D-IR data, we conclude that rapid energy transfer processes occur between base and backbone, mediated by additional modes located on the deoxyribose moiety within the same nucleotide. These relaxation dynamics are insensitive to duplex melting, showing that efficient intramolecular energy relaxation to the solvent via the phosphate groups is the key to excess energy dissipation in both single and double-stranded DNA.

Introduction

Deoxyribonucleic acid (DNA) is the most fundamental of biological molecules. Despite considerable efforts since the structure of the double helix was first determined in 1953 however,¹ questions regarding the relationship between the solution phase molecular physics of DNA and its biological function remain unanswered. For example, the manner in which disparate aspects of the DNA structure (base pairing and stacking; deoxyribose rings; phosphodiester groups) combine cooperatively to stabilize double helical DNA or contribute to duplex unwinding in transcription and replication are not clear. These inter and intramolecular interactions also influence the dynamic landscape of DNA and variations in molecular dynamics with base sequence are believed to underpin fundamental biological processes such as protein-DNA interactions and the recognition of damaged DNA bases. This is manifest in the action of anti-sense therapeutics where the subtle interplay of backbone and base influence efficacy through control of solvation and binding strength respectively.²

The dynamics of vibrational relaxation, relating to mode-mode energy migration and efficient energy dissipation are linked to the naturally short non-radiative lifetimes of DNA excited states and may contribute to the prevention of extensive DNA-damage following electronic-excitation and relaxation.³⁻⁵ Ultrafast spectroscopy has provided considerable insights into the dynamics of electronically-excited DNA,⁶⁻¹¹ including investigations using time-resolved IR spectroscopy on adenine and thymine systems,^{5,12} but the precise relaxation pathways remain to be clearly elucidated.

There exists a clear need to observe, experimentally, the dynamics as well as the structure of DNA in a whole molecule manner, but this brings considerable challenges because, although powerful, time resolved optical spectroscopic methods are often limited by available technology to probing specific, relatively localized aspects of the molecule.

Studies of ground state dynamics have revealed the importance of delocalized phenomena centered on the DNA bases: 2D-IR spectroscopy of carbonyl stretching modes of double-stranded (ds)-GC sequences established that inter-strand vibrational couplings due to W-C H-bonding outweigh those occurring along the strand due to base-stacking interactions.^{13,14} Subsequent computational modeling studies identified significant changes in base vibrational modes upon base pairing leading to the formation of new vibrational 'W-C modes' spanning the paired bases.¹⁵⁻¹⁸ Vibrational coupling and related delocalization of modes has been further shown to be present in the vibrational modes of the isolated bases,¹⁹ while studies of the N-H stretching modes show that coupling affects these to a similar degree and vibrational relaxation between the N-H stretching modes and lower-frequency base modes has been reported at low relative humidity.²⁰⁻²⁸

Recently, the dynamics of the phosphate backbone vibrational modes have been determined under carefully-controlled hydration conditions.^{29,30} These experiments show that the phosphate and phosphodiester modes are also coupled and indicate that the primary energy dissipation mechanism of DNA is through solvent interactions of the phosphate group.

The evidence for the importance of vibrational coupling and delocalized phenomena in parts of the DNA structure is clear. However, the degree to which coupling extends be-

tween the purine and pyrimidine modes and the sugar ring modes is not conclusive,^{31,32} yet is of vital importance when considering the mechanism by which the bases and backbone are dynamically-linked in relation to, for example, an energy transfer pathway. Here, we exploit two-color 2D-IR experiments to specifically probe the interaction of vibrational modes located on the bases with those involving the sugar-phosphate backbone under both double- and single-stranded conditions. We reveal for the first time coupling and energy transfer dynamics that span these spatially-disparate groups via mutual interactions with the deoxyribose unit. The structure-specific nature of the results provides an insight into the unique physical processes that arise from the double helix structure.

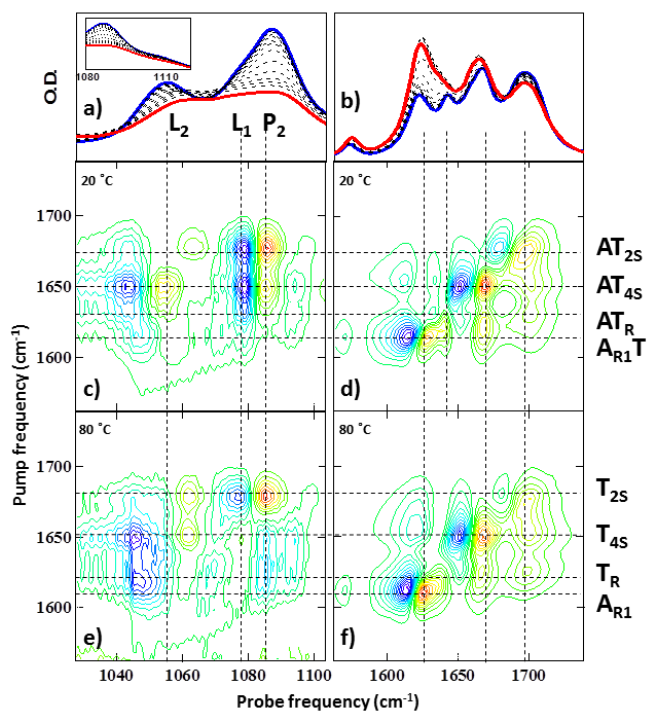


Figure 1: a) IR absorption spectra of AT 15-mer in the backbone stretching region of the spectrum at a range of temperatures from 20 °C (blue) to 80 °C (red). b) IR absorption spectra showing vibrational modes of the bases as a function of temperature. c-f) 2D-IR spectra (ZZYY) showing results of one color (d,f) and two color (c,e) experiments at 20 °C (c,d) and 80 °C (e,f). For vibrational mode definitions, see Fig 2. In all 2D-IR spectra presented, the color scheme runs from red (negative) to blue (positive); contours represent 10% increments in the signal; ‘base’ 2D-IR spectra (d,f) signals cover a range equivalent to ± 10 mOD; ‘base-backbone’ signals were an order of magnitude smaller.

Experimental

Fourier-transform ultrafast 2D-IR spectra were obtained using the pseudo pump-probe geometry method^{33,34} with the LIFETIME spectrometer.^{35,36} Mid-infrared laser pulses were produced by three optical parametric amplifiers (OPA) pumped by two 100 kHz Yb:KGW amplified laser systems, (6W, 180 fs, and 15W, 300 fs) pumping one pump OPA (OPA₁) and two probe OPAs (OPA₂ and OPA₃ respectively). OPA₁ provided the 2D-IR excitation pulses centered near 1650 cm⁻¹, resonant with the base carbonyl/ring stretching modes. OPA₂ provided probe pulses also centered on these base modes (1650 cm⁻¹) for single color ‘base’ 2D-IR experiments while OPA₃ was used in two-color ‘backbone’ 2D-IR experiments to probe the phosphate backbone region of the spectrum near 1070 cm⁻¹. The probe pulse durations pro-

duced by the OPAs were ~ 200 fs. Two co-linear pump pulses, separated by a variable time delay, τ , were created by directing the output of OPA₁ into a mid-IR pulse shaper (Phasetch) and the waiting (pump-probe delay) time was set using an optical delay line situated after the pulse shaper. The pump-pulse duration was ~ 300 fs, which limits the experimental time resolution. The two probe beams were dispersed in separate spectrometers, each equipped with a 128 element MCT array detector. 2D-IR signals were measured using phase cycling and 2D-IR datasets were obtained by scanning τ for a fixed waiting time. Spectra were obtained by Fourier transform along τ . Data was collected in both ZZZZ and ZZZY polarization geometries.

The sample consisted of a 15 base pair oligomer 5' – ATTATTATTATATTA-3' and its complementary sequence (BioTeZ Berlin Buch GmbH) dissolved, without further purification, to a concentration of 10 mM in deuterated tris-buffer (100 mM, pD7.4) containing 100 mM NaCl. Under these conditions, the DNA forms a B-type double helix with a melting temperature of ~ 55 °C, as confirmed by UV-vis and FT-IR absorption spectroscopy (see ESI Figs.S1 and S2). For all IR measurements, the sample was held between two CaF₂ windows separated by a 25 μ m thickness polytetrafluoroethylene spacer and housed in a thermostatically-controlled mount, allowing the temperature to be varied between 20 °C and 80 °C, accurate to ± 1 °C, where the DNA was predominantly in double- and single-stranded conformations respectively.

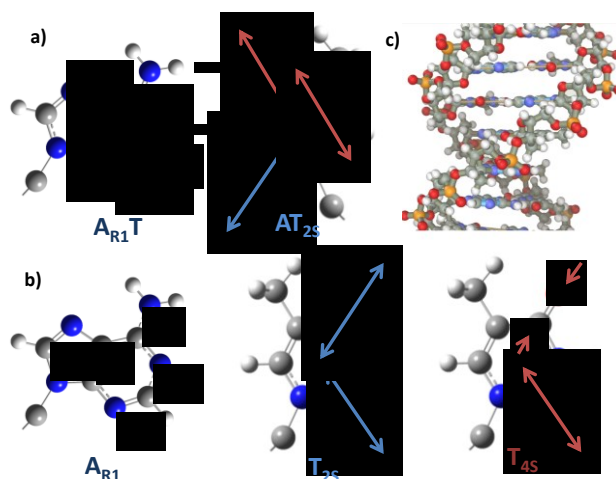


Figure 2: Schematic representation of the vibrational modes of a) W-C base pairs and b) individual bases as used in the text. Descriptions are based on simulations reported in Refs¹⁵⁻¹⁸ c) shows a schematic representation of the ds-AT 15-mer studied in which the bases and sugar-phosphate backbone are visible.

Results

IR spectroscopy: The results of the 2D-IR experiments are shown in Fig.1 alongside temperature-dependent IR absorption spectra. In the ‘base’ region of the IR spectrum near 1650 cm⁻¹, four bands are visible at 20 °C (Fig.1(b) blue spectrum), located at 1692, 1663, 1640 and 1622 cm⁻¹. Following mode designations based on previous computational simulations, these are assigned to the AT_{2S}, AT_{4S}, T_R and A_{R1}T modes of the AT W-C base pair respectively (Fig.2(a)).¹⁵⁻¹⁸ Heating to 80 °C (Fig 1(b) red spectrum) induced a change in the spectrum with three peaks being observed at 1693, 1661 and 1623

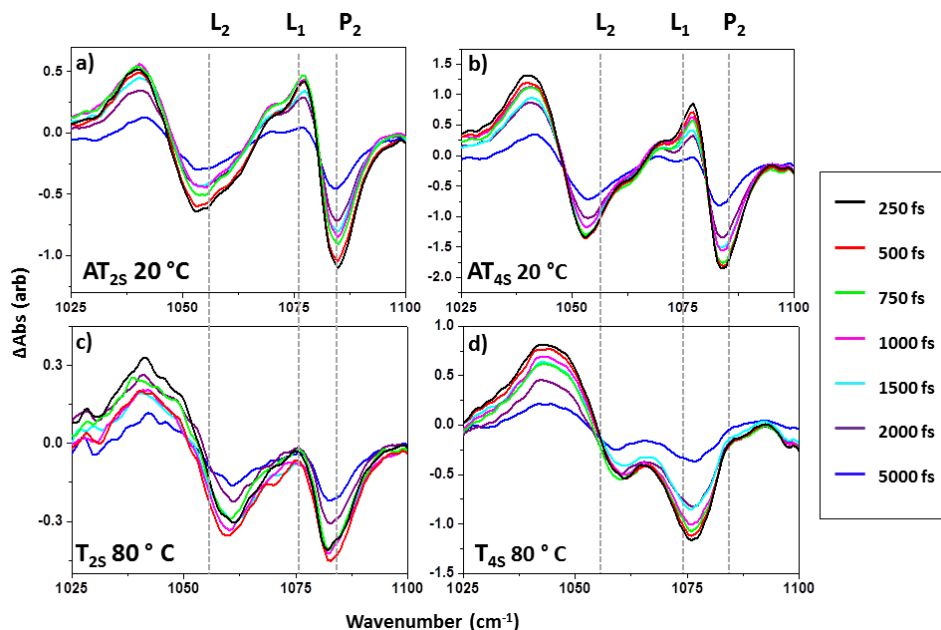


Figure 3: (a-d) Slices taken through 2D-IR spectra of the backbone region at a range of waiting times. Figure legends show identity of excited mode (pump frequency) and temperature in each case. Data has been smoothed using the 7 pt Savitzky-Golay method to remove a low-amplitude modulation on the probe spectrum due to etalon effects caused by the GaSe crystal used for Difference Frequency Generation in OPA3.

T (°C)	Excited Mode	T ₁ (fs)	τ _r (fs)	
			P ₂	L ₂
20	AT _{2S}	550	700	-
	AT _{4S}	850	700	1550
	AT _R	900	750	700
	A _{R1} T	850	1900	600
80	T _{2S}	700	350	-
	T _{4S}	850	-	600
	T _R	-	-	700
	A _{R1}	800	-	-

Table 1: Results of fitting peak dynamics from time-resolved 2D-IR spectroscopy, as described in main text. τ_r values for P₂ peaks represent the average rise times observed for the negative and positive features marked with blue and black arrows in Fig 5 (see text).

cm⁻¹; attributed to the T_{2S}, T_{4S}, and A_{R1} modes of the single-stranded bases respectively (Fig.2(b)).¹⁵⁻¹⁸ A shoulder is also visible at 1632 cm⁻¹ corresponding to the ring-based T_R mode.

In the ‘backbone’ region of the spectrum, near 1070 cm⁻¹, (Fig.1(a)) three bands are observed at both low (blue) and high (red) temperatures; these are assigned to the symmetric PO₂⁻ stretching mode (P₂) located at 1086 cm⁻¹ and the L₁ and L₂ phosphodiester stretching modes at 1075 and 1055 cm⁻¹ respectively.²⁹ The P₁ asymmetric PO₂⁻ stretching mode expected near 1230 cm⁻¹ is obscured by a D₂O solvent transition. A low-intensity feature, located at 1105 cm⁻¹ (inset Fig.1(a)), is assigned to a C1'-C2'-C3'O vibrational mode of the deoxyri-

bose unit.^{34,37} Increasing the temperature resulted in a reduction in the intensity of the P₂ mode, while the L₂ mode shifted slightly to higher wavenumber. Detailed analysis of the IR absorption spectra in both base and backbone regions as a function of temperature (ESI Fig.S2) shows that the changes in both spectral regions are well-represented by a sigmoid-type function with a midpoint near 58 ± 2 °C, consistent with the changes being attributable to helix melting. Fig S2 also shows that FT-IR spectra of the individual ss-DNA sequences used to form the duplex are consistent with that of the melted duplex at 80 °C, confirming that the effect of temperature on the ss-DNA spectroscopy is minimal.

‘Base’ 2D-IR spectroscopy: A representative diagonal 2D-IR spectrum of the base modes, obtained at 20 °C and a waiting time of ~250 fs is shown in Fig.1(d). Negative peaks (red) appear on the spectrum diagonal, corresponding to the ν=0-1 transition of each vibrational mode, with associated positive (blue) ν=1-2 peaks, which are shifted to lower probe frequency by the diagonal anharmonicity of the modes. In light of subsequent discussions focusing on vibrational relaxation, a ‘pump-probe’ description of these spectra has been employed, however it is noted that the signs of the ν=0-1 and ν=1-2 signals are often reversed in photon-echo experiments.

Additional peaks are visible in the off-diagonal region of the spectrum. These are present from the shortest waiting times, showing that all four of the base-pair modes in this spectral region are coupled to one-one-another, consistent with previous computational predictions (Fig.2(a)).¹⁵⁻¹⁸

Heating to 80 °C did not lead to significant changes in the 2D-IR spectrum (Fig.1(f)) of the bases because the 1630 to 1700 cm⁻¹ region is dominated by vibrational modes associated with thymine, and these modes couple similarly in both

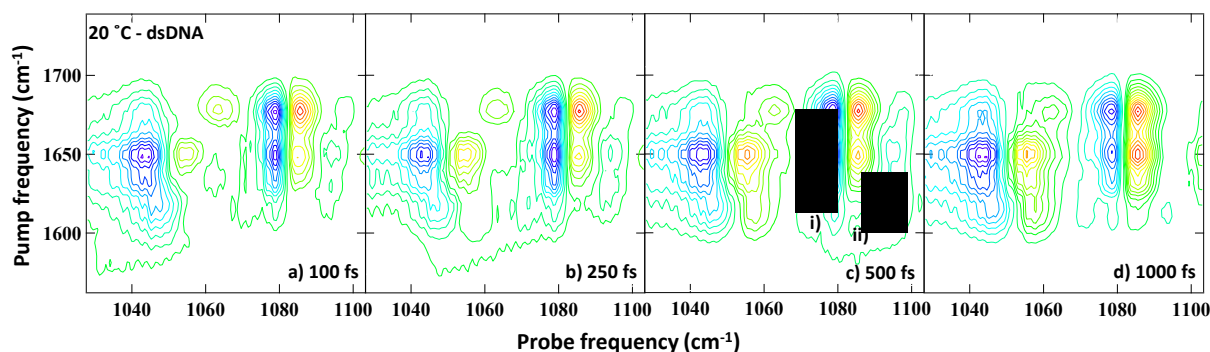


Figure 4: Backbone 2D-IR spectra obtained at a range of waiting times for the ds-DNA sample at 20 °C and ZZZY polarization conditions. The waiting time is given in the individual figure legends. Labels in c) show i) the position of lineshape evolution of the P_2 peak and ii) the $\nu=1-2$ transition of the 1105 cm^{-1} deoxyribose mode as referred to in the text.

ss- and ds-DNA configurations.¹⁵⁻¹⁸ However, careful inspection shows that the T_R mode shifts to lower frequency on going from ds- to ss-DNA and that coupling between A_{R1} and the three T modes is lost upon breaking of the W-C base pairs would be anticipated. Indeed, the coupling patterns observed at 80 °C are very similar to those reported for the individual bases.¹⁹ This result indicates that the interstrand coupling that dominates base vibrational modes in duplex DNA is completely lost when the W-C interaction is broken and is not encouraged through simple solvent-mediated water-phosphate bonding. Thus, the 2D-IR data of these samples further indicates that *inter*-strand coupling of the bases is more dominant than *intra*-strand coupling, in agreement with previous conclusions on dsGC sequences.¹⁴

2D-IR spectra of the bases were obtained as a function of waiting time and peaks were fit to Gaussian lineshape profiles to extract relaxation dynamics (ESI Fig S3(a,b)). The dynamics of the diagonal peaks of both the ds- and ss-DNA configurations were typically well-represented by a single exponential decay function with a timescale of $\sim 750 \pm 200$ fs (see T_1 , Table 1). The $\nu=0-1$ and $\nu=1-2$ transitions showed consistent temporal behavior and good agreement with broadband pump-probe measurements (ESI Fig S4). Neglecting the effects of molecular rotation on these fast timescales, these values are taken to represent the vibrational lifetime (T_1) of the excited modes. The lack of dependence of this parameter upon temperature suggests that the relaxation mechanism of the base modes is not strongly affected by strand conformation or solvent access.

‘Base-Backbone’ 2D-IR spectroscopy: In contrast to the base 2D-IR data, significant changes in the two-color ‘base-backbone’ 2D-IR spectra are observed upon changing the temperature.

Double-stranded DNA: At 20 °C, corresponding to the ds-DNA configuration (Fig 1(c)), off-diagonal peaks were observed to link all four of the excited base W-C vibrational modes to both the P_2 mode of the PO_2^- unit and the L_2 mode of the phosphodiester. Experiments using the perpendicular ZZZY polarization geometry showed changes in amplitude but not in the positions of the peaks observed in the 2D-IR spectra. Fitting cross-sections through the data, such as those shown in Fig.3(a,b), to Gaussian line-shape functions showed that the data was best-represented by a fit that also included peaks linking the base modes with the L_1 mode as well as the P_2 and L_2 modes (ESI Fig S5). With the exception

of excitation of the AT_{2S} mode under ZZZY polarization conditions (Fig.4), where the L_1 peak was more prominent, the L_1 peaks were largely obscured by the strong P_2 and L_2 peaks.

The temporal dynamics of the peaks in the backbone 2D-IR spectra were measured and examples are shown in Fig.4. All peaks were found to be present, albeit of low intensity, at the earliest waiting times (Fig.4(a)). The peaks linking base modes to the L_2 mode for the ds-DNA sample displayed a rise in amplitude. The dynamics recovered for this process were mode-dependent (see τ_r , Table 1) a timescale of 650 ± 100 fs recovered for excitation of AT_R and A_{R1T} ; the AT_{4S-L_2} peak displayed a slower rise time.

In all cases, the rise was followed by a decay that did not show an easily-defined kinetic behavior (eg ESI Fig S6), although fitting the small signal sizes to an exponential decay function suggested a timescale on the order of ~ 10 ps. Extraction of the L_1 relaxation dynamics was found to be problematic due to spectral congestion.

In the case of the off-diagonal peaks linking to the P_2 mode, more complex peak dynamics were observed. In particular, the shape of the features was observed to evolve with waiting time. This is shown in Fig.5(a) via a series of slices through the peak linking P_2 with AT_{4S} that are representative of all of the off-diagonal peaks associated with the P_2 mode in the ds-DNA sample. The negative feature (blue arrow) was observed to follow similar dynamics to those of the L_2 peaks described, with a 700 ± 150 fs rise time observed in the majority of cases. The positive feature however showed two components. At early waiting times, a narrow feature shifted by $\sim 5\text{ cm}^{-1}$ to lower probe frequency dominated the lineshape (red arrow). At longer waiting times this feature decayed and a broader feature centered some 12-15 cm^{-1} to lower probe frequency was observed to grow into the spectrum (black). This process is shown most clearly by comparing the black (waiting time: 0 fs), purple (1500 fs) and orange traces in Fig 5(a), but is also seen in the 2D-IR spectrum (labelled i) in Fig. 4) and in fits to the data (ESI Fig S6). Fig.5(b) shows the early-time dynamics of the three features. Fitting revealed two timescales: The negative (blue arrow) and broad positive (black) features typically shared a 700 ± 150 fs rise time, while the narrow positive feature (red arrow) was observed to increase slightly but with a timescale that lay well within the experimental pulse duration; meaning it is possible only to state that it is clearly present from early waiting times. All peaks show a similar long (~ 10 ps) decay time to the L_2 peaks.

Though partially obscured by the P_2 peaks, a positive feature can be seen in the 2D-IR data at probe frequencies of $\sim 1090\text{ cm}^{-1}$ (labelled (ii) in Fig.4), which was observed to reach a peak amplitude at waiting times of around 500 fs and decay rapidly, disappearing by 1500 fs.

Single-stranded DNA: Increasing the temperature to 80°C and inducing melting of the helix (Fig.1(e)) led to several changes in the spectra, suggesting a fundamental alteration in the nature of the base-backbone interaction. Off-diagonal peaks linking each of the base vibrational modes to the L_2 mode are still observable. However, all off-diagonal peaks linking base modes to the P_2 mode are lost, with the exception of that between the P_2 and T_{2S} modes. This results in the features linking the T_{4S} , T_R and A_{R1} modes to the L_1 mode becoming clearer (Fig.1(e)). These changes can also be seen in cross-sections through the data at excitation frequencies corresponding to the AT_{2S} and AT_{4S} modes (Fig.3(c,d) where the shift in the highest frequency negative feature from a position corresponding to the P_2 mode (Fig.3(c)) to one matching the L_1 (Fig.3(d)) is observable.

Examples of the dynamics of the peaks observed for the ss-DNA sample (80°C) are shown in Fig.6. For ss-DNA, all of the off-diagonal peaks visible in the backbone 2D-IR spectrum were again observed to be present at the earliest waiting times (Fig.6(a)). For off-diagonal peaks linking base modes to the L_2 mode (labelled (i) in Fig.6), similar dynamics were observed to those of the ds-DNA sample: a $\sim 650\text{ fs}$ rise followed by a $\sim 10\text{ ps}$ decay.

The single off-diagonal peak associated with the P_2 mode (labelled (ii) in Fig.6) showed markedly different dynamics in the ss-DNA sample from those in the ds-DNA sample:

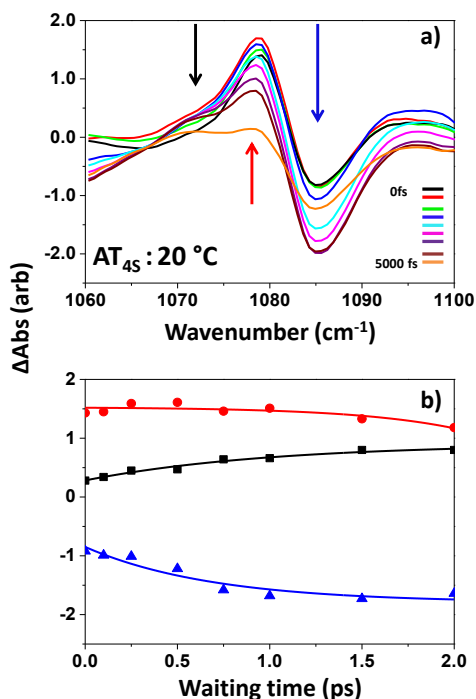


Figure 5: a) Slices through two-color 2D-IR spectra as a function of waiting time showing the peak shape evolution of the off-diagonal peaks to the P_2 mode. b) shows the early-time dynamics of the three components identified by arrows in a). Data in a) has been smoothed as in Fig.3.

The peak shape evolution of the positive features was not observed (Fig.3(c)), instead this feature demonstrated similar rise and decay dynamics to the L_2 peaks, though with a slightly faster rising timescale of 350 fs recovered. The effects of peak overlap prevented reliable extraction of the L_1 dynamics. In addition to these peaks, the positive feature near 1090 cm^{-1} is still clearly visible for the ss-DNA sample (Fig.6, labelled (iii)) and shows similar dynamics at both temperatures studied.

Discussion

The results highlight three main areas of interest: **i)** the assignment of the conformationally-sensitive off-diagonal features in the backbone 2D-IR spectra **ii)** comparisons of the vibrational dynamics between ss- and ds-DNA conformations and **iii)** the marked differences in the observed behavior of off-diagonal peaks to the P_2 mode between ss- and ds-DNA forms.

Off-diagonal peak assignments - coupling: There are three possible assignments for 2D-IR off-diagonal peaks: vibrational coupling of the modes; energy transfer during the elapsed waiting time or chemical exchange.³⁸ Chemical exchange is not applicable in this case, suggesting that the off-diagonal peaks observed in the two-color 2D-IR datasets must arise either from direct coupling of base modes with the phosphate backbone modes and/or energy transfer.

In the event that they arise from vibrational coupling, the off-diagonal features would be expected to appear at the earliest waiting times and the frequency separation of the positive and negative components of the lineshape would be defined by the off-diagonal anharmonicity of the coupled modes (Δ_{ij} ; the shift in energy of the combination band relative to the sum of the energies of the one-quantum excitations).³⁹ For weak couplings, this is manifest as a reduction in overall amplitude of the off-diagonal feature as the two components of the lineshape overlap. In straightforward cases, these features would be expected to decay with the lifetime of the excited mode. In the case of energy transfer, the off-diagonal peak separation reflects the diagonal anharmonicity of the receiving mode, while the amplitude typically follows a rise and decay profile associated with energy transfer and subsequent relaxation dynamics.⁴⁰

The off-diagonal peaks observed in the backbone 2D-IR spectra (Figs.1,4,6) are present from the earliest waiting times. This invites an assignment to coupling. However, the peaks show an amplitude of $<5\%$ of that of the corresponding diagonal peaks, despite similar transition dipole strengths, suggesting that this effect is likely to be very weak ($\Delta_{ij} \leq 1\text{ cm}^{-1}$). In addition, the decay dynamics observed are considerably longer than those of the excited base modes ($\sim 750\text{ fs}$). Vibrational coupling reduces sharply with distance and mode frequency separation and thus direct coupling of the bases to the phosphate modes without a large delocalized vibrational mode structure or close proximity of these features would seem unlikely.⁴⁰ It is also plausible that the fast relaxation of the bases and 300 fs pulse duration employed could combine to give rise to a small signal from energy transfer at very short waiting times, without coupling.

An assignment of the majority of the off-diagonal peaks, in particular those pertaining to the L_1 and L_2 modes, at short waiting times to direct vibrational coupling, while possible, is

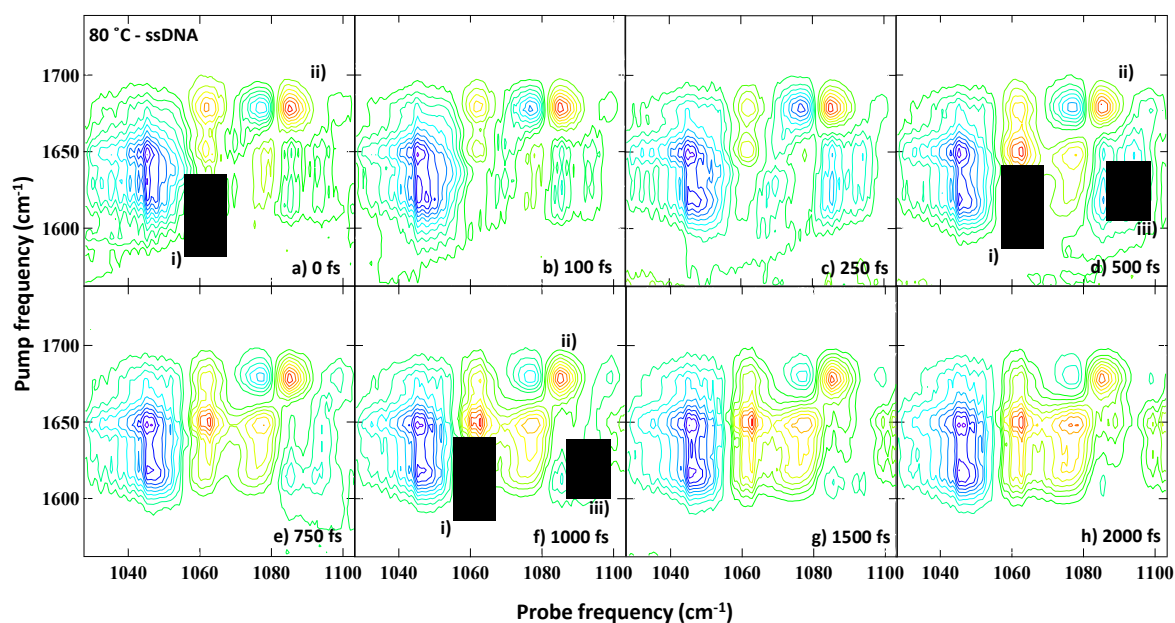


Figure 6: Two-color 2D-IR spectra as a function of waiting time obtained for the ss-DNA sample under ZZZY polarization conditions. The waiting time is quoted in the individual figure legends. Labels in a, d and f show i) the position of the L_2 features that display energy transfer dynamics, ii) the only off-diagonal peak to the P_2 mode that remains in the ss-DNA configuration and iii) the $\nu=1-2$ transition of the 1105 cm^{-1} deoxyribose mode as referred to in the text.

not conclusively proven by the data. It may be considered that the double helix might give rise to the long-range effects that could enable coupling, as seen between carbonyl vibrations in an α -helix for example,⁴¹ however, the persistence of these features at elevated temperature (ss-DNA) is not consistent with this hypothesis. In contrast, some clear changes in the off-diagonal peak patterns upon formation of ds-DNA occur that are specific to the P_2 mode in our dataset. These indicate that the ordered helical structure does in fact influence the coupling of the bases to certain backbone modes and we will return to this in detail below.

Off-diagonal peak assignments – energy transfer:

Under both double and single strand conditions, the majority of the off-diagonal features, with the exception of the narrow positive feature uniquely associated with the P_2 modes in ds-DNA, rise to a maximum within 1-2 ps and then decay. This suggests that an energy transfer mechanism dominates the off-diagonal peak behavior. The close agreement of the timescales of the rising dynamics (~ 650 fs in most cases) with base mode T_1 times could indicate a direct energy transfer pathway, but the peak separations observed for the off-diagonal peak pairs, while similar, are not identical to the diagonal anharmonicities reported from one-color 2D-IR spectroscopy of the phosphate region (See Table S1, ESI).²⁹ This observation is not consistent with direct energy transfer and such a process would normally require significant vibrational coupling or proximity of the modes as well as a mechanism for energy conservation given the large ($\sim 600\text{ cm}^{-1}$) frequency separation of the base and backbone modes.⁴⁰ The vibrational lifetimes of the P_2 , L_1 and L_2 modes were recently reported to be in the region of 1200-2500 fs, which are also inconsistent with the long relaxation dynamics observed for the off-diagonal features.²⁹

An alternative mechanism to explain the temporal behavior of the off-diagonal peaks could involve relaxation of the

base vibrations leading to population transfer to an intermediary mode or modes that are coupled to the backbone modes, giving rise to off-diagonal peaks. Such a situation has been reported in large molecular systems using relaxation-assisted 2D-IR spectroscopy.^{40,42,43} This mechanism would explain the correlation between the rise time of the off-diagonal peaks and T_1 of the base diagonal peaks without direct energy transfer in the first instance. In this case, the off-diagonal peak separation reflects the coupling of the intermediary and backbone modes, which would be expected to differ from the diagonal anharmonicity of the backbone modes. The indication is that population transfer to the backbone modes then follows. This is consistent with the slow decay time of the off-diagonal peaks because multiple energy transfer pathways through the DNA molecule will stretch the timescales for energy flow into backbone modes, with only the fastest being clearly resolved in the peak dynamics. It would be expected that temporal evolution of the lineshape be observed as population transfer to the backbone modes ensued but if diagonal and off-diagonal anharmonicities are similar, or multiple intermediary modes are involved then this may be obscured.

A schematic of the mode patterns for DNA is shown in Fig.7. Whilst many candidates for these intermediary modes exist and would be consistent with evidence from the dynamic data, we suggest no single definitive route is operational. The prospect of structural inhomogeneity along the 15 base strand may also influence the observed dynamics.³⁷ Specific candidate modes include lower frequency modes of the bases and modes of the deoxyribose moiety. In particular, from experiments, lower frequency base modes are known to couple to excited higher frequency modes¹⁹ and coupling of base and sugar ring modes has also been proposed in model systems.^{31,32} It is noteworthy that the sugar moiety has modes with frequencies of around $800\text{-}900\text{ cm}^{-1}$, and these are de-

scribed as being coupled to the phosphodiester moiety.³⁷ The overtone ($\nu=0-2$) transition of the latter modes would match the frequency of the base modes well and could provide an efficient route for relaxation. That they are likely to be coupled to the phosphate group also makes these good candidates for the intermediary modes.

Here it is instructive to note the positive feature with fast rise and decay components that is located to the low frequency side of the 1105 cm^{-1} mode assigned to a deoxyribose vibration (Fig 4, labeled (iii) and Fig 6, labeled (ii)). A comparison of the dynamics of this and peaks to the negative P_2 feature is shown in Fig.8. This feature is located where one would expect an anharmonically-shifted $\nu=1-2$ transition of the 1105 cm^{-1} mode and the fact that it peaks at earlier waiting times than the P_2 and L_2 energy-transfer features and decays faster is entirely consistent with energy transfer from base to sugar prior to onward energy transfer to the backbone. It is noteworthy that the off-diagonal peaks to this feature appear to be dominated by excitation of the lower frequency base modes, involving ring vibrations of A and T, which would be expected to couple more efficiently to sugar modes due to proximity and a slightly narrower energy gap.^{31,32} As such, this experimentally-observed feature supports the proposed mechanism of relaxation from base modes through deoxyribose modes to the phosphate backbone.

An energy cascade model, portrayed in Fig 7 that involves energy transfer from base to sugar is also consistent with IR pump-anti-Stokes Raman probe studies reported on AT systems at 0% relative humidity, which showed that N-H stretching modes relax by populating other base vibrational modes in the $1660-1490\text{ cm}^{-1}$ region of the spectrum within 1 ps and lower frequency modes near 1330 cm^{-1} on 1-2 ps timescales, which subsequently decayed over timescales greater than 5 ps.²⁷ The latter mode was not assigned but could be a low frequency base mode or a mode partially located on the sugar moiety and would be a candidate accepting mode in our model.³⁷

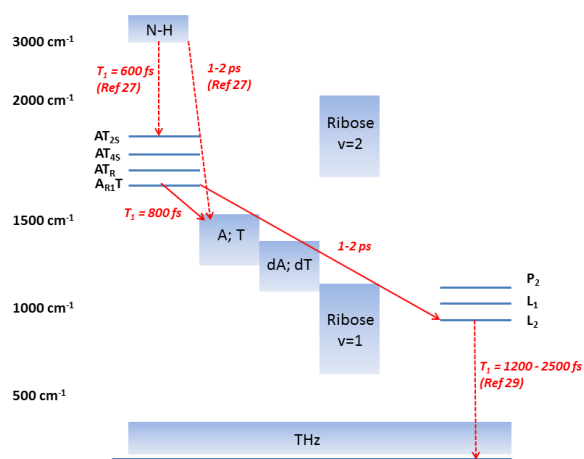


Figure 7: Schematic diagram showing relative positions of DNA vibrational modes. Assignments as per Ref³⁷. Solid arrows show results from this work, dashed arrows show results from prior publications.

Conformation-dependence of Relaxation dynamics: The clear conclusion from the dynamic data is that the relaxation processes of the peaks observed show very little varia-

tion with DNA conformation; that of ss-DNA is very similar to ds-DNA.

The fact that the dynamics of peaks to the L_2 mode and some components of the P_2 mode peaks (the negative and broad positive features shown by the blue and black arrows in Fig.5(a)) are largely invariant with DNA configuration suggests that the dominant energy relaxation mechanism is common to both ds- and ss-DNA and rules out direct involvement of configuration-dependent routes involving solvent modes. On this basis we conclude that the increased solvent access to the bases, in particular the amino and carbonyl units, is not a rate determining step in the overall relaxation mechanism. Overall, our findings are in agreement with the “downhill” transfer of energy towards the backbone in solvated DNA,²⁹ supporting the hypothesis that the fast energy dissipation mechanism acts to prevent damage in electronically excited ss- and ds-DNA.

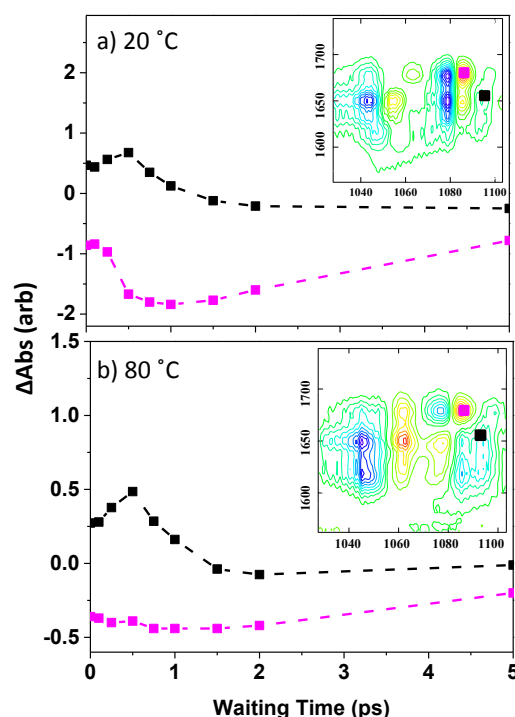


Figure 8: a) Shows relative dynamics of P_2 off-diagonal feature (magenta) and peak assigned to $\nu=1-2$ transition of deoxyribose vibrational mode located at 1105 cm^{-1} (black) at $20\text{ }^\circ\text{C}$ (ds-DNA). The peak positions are marked on the 2D-IR spectra in the insets. Note the faster rise and decay of the black trace relative to the magenta. b) As a) but at $80\text{ }^\circ\text{C}$ (ss-DNA).

P_2 mode dynamics: We now discuss further the structure-dependent behavior of the off-diagonal peaks linking to the P_2 mode. That is; at elevated temperatures (ss-DNA), only a single off-diagonal peak is seen linking P_2 to the AT_{25} base mode (Fig.1(e)), whilst at low temperatures (ds-DNA) off-diagonal peaks are observed linking all four base modes to the P_2 transition (Fig.1(c)). The latter features are unique to the ds-DNA sample and show a complex peak-shape evolution with waiting time (Fig.5(a)). Specifically, a narrow component observed at short waiting times is joined by a broader, red-shifted peak at later times. This behavior is consistent

with evolution from off-diagonal (i.e. coupled) character to diagonal (i.e. energy transfer) character.^{39,40}

The broad feature (Fig.5(a) black arrow) behaves consistently with this model in that it shows very similar dynamics to L_2 mode peaks, suggesting that it is also attributable to the common energy transfer process from base to backbone. Whilst we assign this broad peak to the $\nu=1-2$ transition of the P_2 band,²⁹ the complexity of this spectral region is further highlighted by studies of the $H_2PO_4^-$ ion, which identify a Fermi resonance with the OPO bending vibration in the same spectral region.⁴⁴

By contrast to the broad feature, the narrow 'off-diagonal' component of the P_2 lineshape ((Fig.5(a), red arrow)) is very different to these energy-transfer features and strongly suggests a coupling interaction. The narrow peak is clearly present from the earliest waiting times and the smaller anharmonic shift is consistent with a new coupling interaction arising from the formation of the double helix that gives way to the energy transfer features with increased waiting time. This suggests that the base modes are coupled to the phosphate group by the creation of the W-C modes that accompany ds-DNA formation. The implication is that the new delocalized modes formed by the W-C interaction, which extend over a greater spatial range than the more isolated base modes, lead to further delocalized interactions within the helix that include the deoxyribose units and the phosphate backbone. This agrees with, but significantly extends, predictions of interactions between base and deoxyribose ring vibrations,^{18,24} and leads to the possibility of delocalized helix-specific modes.

The P_2 mode in IR absorption experiments undergoes a significant decrease in intensity upon duplex melting (Fig.1(a)) that cannot be attributed to broadening at increased temperature. One interpretation based on the 2D-IR results is that the loss of intensity stems from changes in the excitonic vibrational coupling of transition dipole moments as found for the α -helix in peptide units.³⁸ In predictions of the IR spectroscopy of B-form AT sequences, it has been shown that significant coupling between T_{4S} and A_{R1} modes leads to spatially delocalized exciton states in double helical strands.¹⁵ This is consistent with the peaks observed in the base 2D-IR spectra (Fig.1(d)). In contrast to the α -helix, the carbonyl modes of the W-C base pair align perpendicular to the axis of the helix. As the P_2 transition dipole moments will align approximately parallel to the base pair axis (ESI Fig.S7), this would seem to favor an interaction with base pair modes that would extend the coupling to the backbone. In support of this, the off-diagonal peak observed between the AT_{4S} mode (which is involved in base pairing) and the P_2 mode is more intense than that from the AT_{2S} mode (not involved in base pairing) under ZZZZ (parallel) polarization conditions; but this is reversed for ZZZY (perpendicular) polarization, indicating an alignment of base W-C modes and phosphate modes in ds-DNA.

Overall, the indication of these observations is that a new set of couplings occurs in ds-DNA, which link the base modes and the P_2 mode of the phosphate group. This opens up a new energy transfer pathway that did not exist in the ss-DNA sample, with the exception of the T_{2S} mode and so augments the energy transfer process observed, particularly for the L_2 mode that is present in both ds- and ss-DNA. The differing structural arrangement of the bases, sugars and

backbone in the double helix thus opens up additional, though not apparently faster, routes for energy relaxation. This would correlate with the loss of other degrees of freedom associated with formation of the helix structure, but implies that the rate determining step is still the transfer of energy from the base modes to other, lower frequency base modes and the deoxyribose unit.

In considering the unusual behavior of the T_{2S} mode, which retains an energy transfer interaction with the bases in ss-DNA (Fig.6, labelled ii), it is perhaps of relevance that this carbonyl does not engage in W-C H-bonding and, in the ds-DNA configuration, is protected from solvated water by projecting into the hydrophobic minor groove. This leads to a closer approach between the T_2 carbonyl and the phosphate backbone in the ds-DNA sample and the fact that the energy transfer process remains upon melting of the helix implies that there may be some element of this interaction, perhaps linked to persistent hydrophobic effects, that remains in the ss-DNA sample independent of the helix formation. Crucially, the aspect of the P_2 off-diagonal peaks assigned to helix-specific coupling is not seen in the ss-DNA sample.

Conclusions

2D-IR spectroscopy has revealed for the first time, the existence of ultrafast energy transfer processes linking vibrational modes of the bases with those of the phosphodiester backbone in both ss- and ds-DNA.

Our results show that vibrational energy dissipation from the bases proceeds via relaxation to populate lower frequency modes, some of which are located on the deoxyribose groups, which are coupled to the phosphate backbone. This is an intermediate step to vibrational population transfer to the backbone modes. It is determined that the dynamics of this mechanism are largely invariant upon melting of ds-DNA, consistent with the hypothesis that the phosphate groups are the primary energetic link between DNA and the solvent.^{25,29}

Formation of ds-DNA leads to new mode coupling patterns between base and backbone, specifically linking base vibrations to symmetric stretch of the phosphate group, suggesting that the delocalization of vibrational modes occurring in W-C H-bonding is extended in the double helix. The indication of interactions spanning base and backbone raises questions of whether these are base or sequence specific and so could relate to long-range dynamic processes that play a role in recognition or excited state energy dissipation. It is to be hoped that these data will stimulate further theoretical or computational simulation of this important molecule.

Author Information

Corresponding Author

neil.hunt@strath.ac.uk Tel: +44 (0)141 5483763

Acknowledgment

The authors wish to acknowledge funding from the STFC (ST/M000125/1 and NTH Programme Access funding), BBSRC (BB/L014335/1) and EPSRC, (University of Strathclyde Doctoral training grant), which supported this work.

Associated Content

Supporting Information Available

Additional electronic content shows supplementary supporting FT-IR, UV-vis and pump-probe spectroscopy data along with additional figures showing data fitting results. This information is available free of charge via the internet at <http://pubs.acs.org>

References

- (1) Watson, J. D.; Crick, F. H. C. Molecular Structure of Nucleic Acids - A Structure for Deoxyribose Nucleic Acid, *Nature* **1953**, *171*, 737-738.
- (2) Krieg, A. M.; Yi, A. K.; Matson, S.; Waldschmidt, T. J.; Bishop, G. A.; Teasdale, R.; Koretzky, G. A.; Klinman, D. M. CpG Motifs in Bacterial-DNA Trigger Direct B-cell Activation, *Nature* **1995**, *374*, 546-549.
- (3) Kuimova, M. K.; Cowan, A. J.; Matousek, P.; Parker, A. W.; Sun, X. Z.; Towrie, M.; George, M. W. Monitoring the Direct and Indirect Damage of DNA Bases and Polynucleotides by using Time-resolved Infrared Spectroscopy, *Proc Nat Acad Sci* **2006**, *103*, 2150-2153.
- (4) Kuimova, M. K.; Dyer, J.; George, M. W.; Grills, D. C.; Kelly, J. M.; Matousek, P.; Parker, A. W.; Sun, X. Z.; Towrie, M.; Whelan, A. M. Monitoring the Effect of Ultrafast Deactivation of the Electronic Excited States of DNA Bases and Polynucleotides following 267 nm Laser Excitation using Picosecond Time-resolved Infrared Spectroscopy, *Chemical Communications* **2005**, 1182-1184.
- (5) Towrie, M.; Doorley, G. W.; George, M. W.; Parker, A. W.; Quinn, S. J.; Kelly, J. M. ps-TRIR covers all the Bases - Recent Advances in the use of Transient IR for the Detection of Short-lived Species in Nucleic Acids, *Analyst* **2009**, *134*, 1265.
- (6) Middleton, C. T.; de La Harpe, K.; Su, C.; Law, Y. K.; Crespo-Hernandez, C. E.; Kohler, B. In *Ann Rev Phys Chem* 2009; Vol. 60, p 217-239.
- (7) Schreier, W. J.; Schrader, T. E.; Koller, F. O.; Gilch, P.; Crespo-Hernandez, C. E.; Swaminathan, V. N.; Carell, T.; Zinth, W.; Kohler, B. Thymine Dimerization in DNA is an Ultrafast Photoreaction, *Science* **2007**, *315*, 625-629.
- (8) Perun, S.; Sobolewski, A. L.; Domcke, W. Ab initio Studies on the Radiationless Decay Mechanisms of the Lowest Excited Singlet States of 9H-adenine, *J Am Chem Soc* **2005**, *127*, 6257-6265.
- (9) Kang, H.; Lee, K. T.; Jung, B.; Ko, Y. J.; Kim, S. K. Intrinsic Lifetimes of the Excited State of DNA and RNA Bases, *J Am Chem Soc* **2002**, *124*, 12958-12959.
- (10) Pecourt, J. M. L.; Peon, J.; Kohler, B. DNA Excited-state Dynamics: Ultrafast Internal Conversion and Vibrational Cooling in a Series of Nucleosides, *J Am Chem Soc* **2001**, *123*, 10370-10378.
- (11) Pecourt, J. M. L.; Peon, J.; Kohler, B. Ultrafast Internal Conversion of Electronically Excited RNA and DNA Nucleosides in Water, *J Am Chem Soc* **2000**, *122*, 9348-9349.
- (12) Doorley, G. W.; Wojdyla, M.; Watson, G. W.; Towrie, M.; Parker, A. W.; Kelly, J. M.; Quinn, S. J. Tracking DNA Excited States by Picosecond-Time-Resolved Infrared Spectroscopy: Signature Band for a Charge-Transfer Excited State in Stacked Adenine-Thymine Systems, *Journal of Physical Chemistry Letters* **2013**, *4*, 2739-2744.
- (13) Krummel, A. T.; Zanni, M. T. DNA Vibrational Coupling Revealed with Two-dimensional Infrared Spectroscopy: Insight into why Vibrational Spectroscopy is Sensitive to DNA Structure, *J Phys Chem B* **2006**, *110*, 13991-14000.
- (14) Krummel, A. T.; Mukherjee, P.; Zanni, M. T. Inter and Intrastrand Vibrational Coupling in DNA Studied with Heterodyned 2D-IR Spectroscopy, *J Phys Chem B* **2003**, *107*, 9165-9169.
- (15) Lee, C.; Cho, M. Vibrational Dynamics of DNA : IV. Vibrational Spectroscopic Characteristics of A-, B-, and Z-form DNAs, *J Chem Phys* **2007**, *126*, 145102.
- (16) Lee, C.; Park, K.-H.; Kim, J.-A.; Hahn, S.; Cho, M. Vibrational Dynamics of DNA. III. Molecular Dynamics Simulations of DNA in Water and Theoretical Calculations of the Two-dimensional Vibrational Spectra, *J Chem Phys* **2006**, *125*, 114510.
- (17) Lee, C.; Park, K.-H.; Cho, M. Vibrational Dynamics of DNA. I. Vibrational Basis Modes and Couplings, *J Chem Phys* **2006**, *125*, 114508.
- (18) Lee, C.; Cho, M. Vibrational Dynamics of DNA. II. Deuterium Exchange Effects and Simulated IR Absorption Spectra, *J Chem Phys* **2006**, *125*, 114509.
- (19) Peng, C. S.; Jones, K. C.; Tokmakoff, A. Anharmonic Vibrational Modes of Nucleic Acid Bases Revealed by 2D IR Spectroscopy, *J Am Chem Soc* **2011**, *133*, 15650-15660.
- (20) Greve, C.; Preketes, N. K.; Fidler, H.; Costard, R.; Koeppel, B.; Heisler, I. A.; Mukamel, S.; Temps, F.; Nibbering, E. T. J.; Elsaesser, T. N-H Stretching Excitations in Adenosine-Thymidine Base Pairs in Solution: Pair Geometries, Infrared Line Shapes, and Ultrafast Vibrational Dynamics, *J Phys Chem A* **2013**, *117*, 594-606.
- (21) Szyz, L.; Yang, M.; Nibbering, E. T. J.; Elsaesser, T. Ultrafast Vibrational Dynamics and Local Interactions of Hydrated DNA, *Angew Chemie Int Ed* **2010**, *49*, 3598-3610.
- (22) Greve, C.; Preketes, N. K.; Costard, R.; Koeppel, B.; Fidler, H.; Nibbering, E. T. J.; Temps, F.; Mukamel, S.; Elsaesser, T. N-H Stretching Modes of Adenosine Monomer in Solution Studied by Ultrafast Nonlinear Infrared Spectroscopy and Ab Initio Calculations, *J Phys Chem A* **2012**, *116*, 7636-7644.
- (23) Yang, M.; Szyz, L.; Elsaesser, T. Femtosecond Two-Dimensional Infrared Spectroscopy of Adenine-Thymine Base Pairs in DNA Oligomers, *J Phys Chem B* **2011**, *115*, 1262-1267.
- (24) Yang, M.; Szyz, L.; Elsaesser, T. Decelerated Water Dynamics and Vibrational Couplings of Hydrated DNA Mapped by Two-Dimensional Infrared Spectroscopy, *J Phys Chem B* **2011**, *115*, 13093-13100.
- (25) Szyz, L.; Yang, M.; Elsaesser, T. Ultrafast Energy Exchange via Water-Phosphate Interactions in Hydrated DNA, *J Phys Chem B* **2010**, *114*, 7951-7957.
- (26) Szyz, L.; Dwyer, J. R.; Nibbering, E. T. J.; Elsaesser, T. Ultrafast dynamics of N-H and O-H stretching excitations in hydrated DNA oligomers, *Chem Phys* **2009**, *357*, 36-44.
- (27) Kozich, V.; Szyz, L.; Nibbering, E. T. J.; Werncke, W.; Elsaesser, T. Ultrafast Redistribution of Vibrational Energy after Excitation of NH Stretching Modes in DNA Oligomers, *Chem Phys Lett* **2009**, *473*, 171-175.
- (28) Dwyer, J. R.; Szyz, L.; Nibbering, E. T. J.; Elsaesser, T. Ultrafast Vibrational Dynamics of Adenine-thymine Base Pairs in DNA Oligomers, *J Phys Chem B* **2008**, *112*, 11194-11197.
- (29) Siebert, T.; Guchhait, B.; Liu, Y.; Costard, R.; Elsaesser, T. Anharmonic Backbone Vibrations in Ultrafast Processes at the DNA-Water Interface, *J Phys Chem B* **2015**, *119*, 9670-9677.
- (30) Guchhait, B.; Liu, Y.; Siebert, T.; Elsaesser, T. Ultrafast Vibrational Dynamics of the DNA Backbone at Different Hydration Levels Mapped by Two-dimensional Infrared Spectroscopy, *Struct dyn* **2016**, *3*, 043202-043202.
- (31) Pelmeshnikov, A.; Hovorun, D. M.; Shishkin, O. V.; Leszczynski, J. A Density Functional Theory Study of Vibrational Coupling between Ribose and Base Rings of Nucleic Acids with Ribosyl Guanosine as a Model System, *J Chem Phys* **2000**, *113*, 5986-5990.
- (32) Toyama, A.; Takino, Y.; Takeuchi, H.; Harada, I. Ultraviolet Resonance Raman-spectra of Ribosyl c(1')-deuterated Purine Nucleosides - Evidence of Vibrational Coupling between Purine and Ribose Rings, *J Am Chem Soc* **1993**, *115*, 11092-11098.

- (33) Deflores, L. P.; Nicodemus, R. A.; Tokmakoff, A. Two Dimensional Fourier Transform Spectroscopy in the Pump-probe Geometry, *Opt Lett* **2007**, *32*, 2966-2968.
- (34) Shim, S. H.; Strasfeld, D. B.; Ling, Y. L.; Zanni, M. T. Automated 2D IR Spectroscopy using a Mid-IR Pulse Shaper and Application of this Technology to the Human Islet Amyloid Polypeptide, *Proc Nat Acad Sci* **2007**, *104*, 14197-14202.
- (35) Donaldson, P. M.; Greetham, G. M.; Shaw, D. J.; Parker, A. W.; Towrie, M. A 100 kHz Pulse Shaping 2D-IR Spectrometer based on Yb:KGW Amplifiers, *Opt Lett* **2016**, *submitted*.
- (36) Greetham, G. M.; Donaldson, P. M.; Nation, C.; Sazanovich, I. V.; Clark, I. P.; Shaw, D. J.; Parker, A. W.; Towrie, M. A 100 kHz Time-Resolved Multiple-Probe Femtosecond to Second IR Absorption Spectrometer., *Appl Spectrosc* **2016**, *doi: 10.1177/0003702816631302*.
- (37) Banyay, M.; Sarkar, M.; Graslund, A. A Library of IR Bands of Nucleic Acids in Solution, *Biophysical Chemistry* **2003**, *104*, 477-488.
- (38) Hamm, P.; Zanni, M. T. *Concepts and Method of 2D Infrared Spectroscopy*; Cambridge University Press: Cambridge, 2011.
- (39) Rubtsov, I. V.; Hochstrasser, R. M. Vibrational Dynamics, Mode Coupling, and Structural Constraints for Acetylproline-NH₂, *J Phys Chem B* **2002**, *106*, 9165-9171.
- (40) Rubtsova, N. I.; Rubtsov, I. V. In *Annual Review of Physical Chemistry, Vol 66*; Johnson, M. A., Martinez, T. J., Eds. 2015; Vol. 66, p 717-738.
- (41) Fang, C.; Wang, J.; Kim, Y. S.; Charnley, A. K.; Barber-Armstrong, W.; Smith, A. B.; Decatur, S. M.; Hochstrasser, R. M. Two-dimensional Infrared Spectroscopy of Isotopomers of an Alanine Rich Alpha-helix, *J Phys Chem B* **2004**, *108*, 10415-10427.
- (42) Naraharisetty, S. R. G.; Kasyanenko, V. M.; Rubtsov, I. V. Bond Connectivity Measured via Relaxation-assisted Two-dimensional Infrared Spectroscopy *J Chem Phys* **2008**, *128*, 104502.
- (43) Kurochkin, D. V.; Naraharisetty, S. R. G.; Rubtsov, I. V. A Relaxation-assisted 2D IR Spectroscopy Method, *Proc Nat Acad Sci* **2007**, *104*, 14209-14214.
- (44) Costard, R.; Tyborski, T.; Fingerhut, B. P. Anharmonicities and Coherent Vibrational Dynamics of Phosphate Ions in Bulk H₂O, *PhysChemChemPhys* **2015**, *17*, 29906-29917.

